

The Deuteron Tensor Structure Function b_1

(A Letter-of-Intent to Jefferson Lab PAC-37)

J.-P. Chen, P. Solvignon[†]

Thomas Jefferson National Accelerator Facility, Newport News VA, 23606

N. Kalantarians, O. Rondon

University of Virginia, Charlottesville, VA, Charlottesville, VA 22903

K. Slifer

University of New Hampshire, Durham NH, 03861

Abstract

Inclusive scattering from a spin-1 target is described by eight structure functions. Four of these, the so-called tensor structure functions, do not exist in the case of a spin-1/2 target. Until now, tensor structure has been largely unexplored, so the study of these quantities holds the potential of initiating a new field of spin physics. In particular, the EMC experiment revealed that only a small fraction of the nucleon spin is carried by valence quarks. Two decades later, the ‘spin crisis’ remains an open issue. Quark orbital angular momentum is now considered to be one of the principal contributions in generating the nucleon spin, but a precise determination of this critical piece has been elusive. The leading twist tensor structure function b_1 can provide new insight into this puzzle, since b_1 can be directly connected to effects arising from orbital angular momentum: b_1 vanishes for the case of the deuteron constituents in a relative S state. For this reason, it provides a unique tool to study strictly partonic effects, while also being sensitive to cumulative nuclear properties, such as the in-medium modification of the nucleon substructure, and the EMC effect. Depending on the choice of Bjorken variable, two disparate phenomena can be explored via measurement of b_1 . At low x , shielding/anti-shielding effects are expected to dominate, while at high x , b_1 can provide one clean way to study ‘Novel QCD effects’; for example, hidden color due to 6-quark configuration. Since the D-state contribution to the deuteron wave function is relatively well known, any novel effects should be readily observable.

We propose a measurement of the deuteron tensor asymmetry A_{zz} , and extract b_1 in the region $0.05 < x < 0.60$, for $1.0 < Q^2 < 5.0 \text{ GeV}^2$. This will provide access to the tensor quark polarization, and allow a test of the Close-Kumano sum rule. A polarized solid ^6LiD target will be utilized along with the Hall A SoLID spectrometer, and an unpolarized 100 nA, 11 GeV incident beam during a 38 day measurement.

[†]Contact person: solvigno@jlab.org

Contents

1	Tensor Structure Functions	3
1.1	The Operator Product Expansion	3
1.2	The Parton Model	4
1.3	Further Theoretical Interpretations	4
1.3.1	Conventional Nuclear Effects	5
1.3.2	Double-Scattering Effects	6
1.3.3	The Close-Kumano Sum Rule	6
1.4	Comments from Theorists	6
2	Existing Data	8
3	The Proposed Experiment	11
3.1	Overhead	12
3.2	Background	13
3.3	Experimental Method	13
3.4	Systematic Uncertainties	14
3.5	Alternate Methodology	14
3.6	Polarized Target	14
4	Summary	16
A	Feasibility Study in Hall C with the HMS and SHMS Spectrometers	17
A.1	Overhead	18
A.2	Background	19
A.3	Experimental Method	19
A.4	Conclusion	19

1 Tensor Structure Functions

The tensor polarized structure of the deuteron was first discussed for the real photon case by Pais [1] in 1967 and later, in the virtual photon case, by Frankfurt and Strikman [2]. In 1988, Hoodbhoy, Jaffe and Manohar [3] introduced the notation which we follow in this letter, whereby the tensor structure is described by the four functions b_1 , b_2 , b_3 and b_4 .

For a spin-1/2 target and after requiring parity and time reversal invariance, only four independent helicity amplitudes are necessary to describe virtual Compton scattering. This number doubles in the case of a spin-1 target as the spin can be in three states (+, 0, -). The hadronic tensor can therefore be decomposed into eight independent structure functions:

$$\begin{aligned}
 W_{\mu\nu} = & -F_1 g_{\mu\nu} + F_2 \frac{P_\mu P_\nu}{\nu} \\
 & -b_1 r_{\mu\nu} + \frac{1}{6} b_2 (s_{\mu\nu} + t_{\mu\nu} + u_{\mu\nu}) \\
 & + \frac{1}{2} b_3 (s_{\mu\nu} - u_{\mu\nu}) + \frac{1}{2} b_4 (s_{\mu\nu} - t_{\mu\nu}) \\
 & + i \frac{g_1}{\nu} \epsilon_{\mu\nu\lambda\sigma} q^\lambda s^\sigma + i \frac{g_2}{\nu^2} \epsilon_{\mu\nu\lambda\sigma} q^\lambda (p \cdot q s^\sigma - s \cdot q p^\sigma)
 \end{aligned} \tag{1}$$

The expressions of $r_{\mu\nu}$, $s_{\mu\nu}$, $t_{\mu\nu}$ and $u_{\mu\nu}$ can be found in [3]. They all contain terms proportional to the polarization of the target E . The structure functions F_1 , F_2 , g_1 and g_2 have the same expressions and are measured the same way as for a spin-1/2 target. The spin-dependent structure functions b_1 , b_2 , b_3 , b_4 are symmetric under $\mu \leftrightarrow \nu$ and $E \leftrightarrow E^*$ and therefore can be isolated from F_1 and g_1 by unpolarized beam scattering of a polarized spin-1 target.

1.1 The Operator Product Expansion

In the Operator Product Expansion (OPE) framework, the leading operators $O_V^{\mu_1 \dots \mu_n}$ and $O_A^{\mu_1 \dots \mu_n}$ in the expansion are twist two. For a spin-1 target, the matrix elements of the time-ordered product of two currents $T_{\mu\nu}$ have the following expressions:

$$\begin{aligned}
 \langle p, E | O_V^{\mu_1 \dots \mu_n} | p, E \rangle &= S[a_n p^{\mu_1} \dots p^{\mu_n} + d_n (E^{*\mu_1} E^{\mu_2} - \frac{1}{3} p^{\mu_1} p^{\mu_2}) p^{\mu_3} \dots p^{\mu_n}], \\
 \langle p, E | O_A^{\mu_1 \dots \mu_n} | p, E \rangle &= S[r_n \epsilon^{\lambda\sigma\tau\mu_1} E_\lambda^* E_\sigma p_\tau p^{\mu_2} \dots p^{\mu_n}]
 \end{aligned} \tag{2}$$

The non-zero value of b_1 arises from the fact that, in a spin-1 target, the $\frac{1}{3} p^{\mu_1} p^{\mu_2}$ doesn't cancel the tensor structure $E^{*\mu_1} E^{\mu_2}$. The coefficient d_n can be extracted from the comparison of $T_{\mu\nu}$ expansion and the spin-1 target hadronic tensor Eq. 1 as follows:

$$\begin{aligned}
 b_1(\omega) &= \sum_{n=2,4,\dots}^{\infty} 2C_n^{(1)} d_n \omega^n, \\
 b_2(\omega) &= \sum_{n=2,4,\dots}^{\infty} 4C_n^{(2)} d_n \omega^{n-1},
 \end{aligned} \tag{3}$$

for $1 \leq |\omega| \leq \infty$ (where $\omega = 1/x$). A Callan-Gross-type relation exists for between the two leading order tensor structure functions:

$$2xb_1 = b_2 \tag{4}$$

valid at lowest order of QCD, where $C_n^{(1)} = C_n^{(2)}$. At higher orders, Eq. 4 is violated.

Sum rules can be extracted from the moments of the tensor structure functions:

$$\begin{aligned}\int_0^1 x^{n-1} b_1(x) dx &= \frac{1}{2} C_n^{(1)} d_n, \\ \int_0^1 x^{n-2} b_2(x) dx &= C_n^{(2)} d_n,\end{aligned}\tag{5}$$

where n is even.

The OPE formalism is based on QCD and is target-independent. However, a target dependence is generated by Eq. 2, and spin-1 structure functions are subject to the same QCD corrections and their moments have the same anomalous dimensions as for a spin-1/2 target. In addition, the tensor structure functions should exhibit the same scaling behavior as F_1 and F_2 , since they are generated from the same matrix element $O_V^{\mu_1 \dots \mu_n}$.

1.2 The Parton Model

In the infinite momentum frame[‡] of the parton model, the scattering of the virtual photon off a free quark with spin up (or down), which carries a momentum fraction x of the spin- m hadron, can be expressed through the hadronic tensor $W_{\mu\nu}^{(m)}$:

$$W_{\mu\nu}^{(1)} = \left(-\frac{1}{2} g_{\mu\nu} + \frac{x}{\nu} P_\mu P_\nu \right) (q_\uparrow^1(x) + q_\downarrow^1(x)) + \frac{i\epsilon_{\mu\nu\lambda\sigma} q^\lambda s^\sigma}{2\nu} (q_\uparrow^1(x) - q_\downarrow^1(x)),$$

for a target of spin projection equal to 1 along the z -direction, and:

$$W_{\mu\nu}^{(0)} = \left(-\frac{1}{2} g_{\mu\nu} + \frac{x}{\nu} P_\mu P_\nu \right) 2q_\uparrow^0(x)\tag{6}$$

for a target of spin projection equal to zero along the z -direction. The tensor structure functions b_1 and b_2 can be expressed from the comparison of $W_{\mu\nu}^{(1)} - W_{\mu\nu}^{(0)}$ with Eq. 1 as follows:

$$\begin{aligned}b_1(x) &= \frac{1}{2} (2q_\uparrow^0(x) - q_\uparrow^1(x) - q_\downarrow^1(x)) \\ b_2(x) &= 2xb_1(x)\end{aligned}\tag{7}$$

Therefore the tensor structure functions depend of the spin-averaged parton distributions $q^1(x) = q_\uparrow^1(x) + q_\downarrow^1(x)$ and $q^0(x) = q_\uparrow^0(x) + q_\downarrow^0(x) = 2q_\uparrow^0(x)$ (since, by parity, $q_\uparrow^m = q_\downarrow^m$) and measure the difference in partonic constituency in an $m=1$ target and an $m=0$ target.

1.3 Further Theoretical Interpretations

The leading twist tensor structure function b_1 quantifies effects not present in the case of spin-half hadrons. However the only available targets to study the tensor polarization effects on the nucleon substructure are nuclei. A measurement of b_1 would allow us to take a deeper look at the nucleus internal dynamics as b_1 should be zero if the nucleus is made up of spin-half constituents at rest, or in a relative s -wave. Therefore a non-negligible value of b_1 can be understood in terms of the deviation of a nucleus from a simple bound state of protons and neutrons.

[‡]All spins and momenta are along the z -axis.

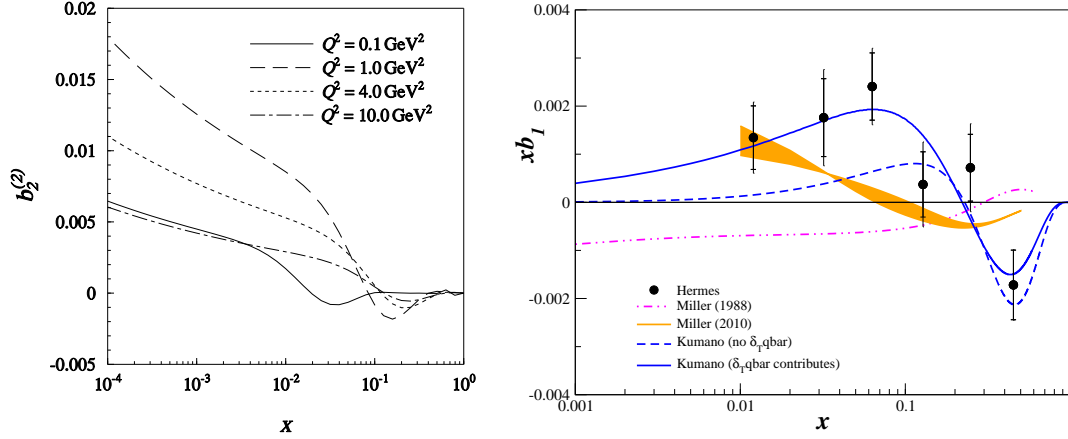


Figure 1: Theoretical predictions. **Left plot:** Double-scattering contribution to $b_2(x, Q^2)$ as a function of x [4]. Note the strong Q^2 dependence at low x . **Right plot:** HERMES results [5] compared to calculations from S. Kumano [6] and from the one-pion exchange effects of G. Miller [7, 8].

1.3.1 Conventional Nuclear Effects

The deuteron is the simplest spin-1 many-body nuclear system. In Ref. [3], the authors evaluate the value of b_1 in three different scenarios for the deuteron constituents and their dynamics:

- I. The deuteron is composed of two spin-1/2 non-interacting nucleons at rest. In this case, the eight helicity amplitudes characteristic of a spin-1 target are expressed in terms of the four helicity amplitudes of each spin-1/2 nucleons, and therefore the total number of independent amplitudes is reduced from eight to four. All structure functions of the deuteron are then the simple sum of the structure functions of the two nucleons, and the tensor structure functions vanish: $b_1 = b_2 = b_3 = b_4 = 0$.
- II. The deuteron is composed of two spin-1/2 nucleons moving non-relativistically in a central potential. The target motion modifies the helicity amplitudes. Using the convolution formalism, it was found that the contribution of these moving nucleons to b_1 is small and is dominated by the lower component of the nucleon's Dirac wave function.
- III. The deuteron contains a D -state admixture. Because the proton and the neutron are moving in opposite directions, an additional term due to the $S - D$ interference appears in the convolution procedure. This extra contribution to b_1 is predicted to be even smaller than in the previous case.

However, at the quark level, when considering the case of massless relativistic quark, b_1 exhibits very large negative values peaked at $x = 0.5$ [3]. In this calculation, a meson in the $j = 1$ state is formed from the coupling of a $P_{3/2}$ massless quark with a spin-1/2 spectator.

In 1988, Miller also examined the tensor structure function b_1 [7]. The basic mechanism is that the virtual photon hits an exchanged pion which is responsible for the binding of the deuteron. The calculation depends on the pion structure function which carries uncertainty. In this early calculation, the convention used by Miller was different from the one used in the HERMES results and in Ref. [6]. The updated calculation [8] is shown in Fig. 1. Also the pion structure function from [9] was used. The spread of the curve originates from the parameter $A_s = (.9 \pm 0.3)$ which governs the strength of the sea in the pion. These

numbers are all in qualitative agreement with HERMES, given their large error bars. Another mechanism is expecting to contribute: coherent-double scattering. Miller specified that his mechanism is not the same as that, even though the HERMES publication [5] combined them together.

In addition, at $x > 0.2$, a non-negligible value of b_1^d is expected just through the conventional nuclear effects in the deuteron, Fermi motion and binding [10].

1.3.2 Double-Scattering Effects

Using Vector Meson Dominance (VMD), the authors of Ref. [4] isolate the double-scattering contribution to b_1 . The existence time of a vector meson can be described by the coherence length λ :

$$\lambda = \frac{Q^2}{Mx(M_v^2 + Q^2)} \quad (8)$$

which is the length over which the vector meson propagates during the time $\Delta t = 1/\Delta E$. Therefore, for multiple scattering to occur, a minimum coherence length of ≈ 1.7 fm (the inter-nucleon separation) is required. At $x > 0.3$, the coherence length is only about the size of the nucleon, so multiple scattering contributions are anticipated to be negligible. However, for $x \leq 0.1$, double-scattering should be significant in b_1 behaving as $(1 - x)^{2\delta}/x^{1+2\delta}$, where δ is determined from the soft pomeron intercept $\alpha_P(t = 0) = 1 + \delta$. Finally the authors foresee a significant enhancement of b_1 at low x (≤ 0.01) due to the quadrupole deformation of the deuteron.

1.3.3 The Close-Kumano Sum Rule

Following the formalism from the parton model in [3], Close and Kumano [11] related the tensor structure function b_1 to the electric quadrupole form factor of the spin-1 target through a sum rule:

$$\begin{aligned} \int_0^1 dx b_1(x) &= -\frac{5}{12M^2} \lim_{t \rightarrow 0} t F_Q(t) + \frac{1}{9} (\delta Q + \delta \bar{Q})_s \\ &= \frac{1}{9} (\delta Q + \delta \bar{Q})_s = 0 \end{aligned} \quad (9)$$

The sum rule is satisfied in the case of an unpolarized sea. However, the authors emphasize that in nucleon-only models the integral of b_1 is not sensitive to the tensor-polarization of the sea, and consequently the sum rule is always true, even when the deuteron is in a D -state.

Recently, Kumano [6] estimated from an analysis of HERMES data [5] that a non-negligible tensor polarization of the sea is necessary to reproduce the trend of the data. However, this conclusion has to be considered with caution due to the large Q^2 coverage of each HERMES data point (see Fig. 4), and the assumption that the sum rule is satisfied for valence quarks.

1.4 Comments from Theorists

During the preparation of this letter, we contacted several theorists to gauge interest in a precision measurement of b_1 . The response was uniformly positive. We provide some of their feedback for context.

“The tensor structure of the deuteron can be investigated in the deep inelastic region by measuring the structure function b_1 , which should shed light on a new aspect of tensor-structure studies in terms of quark

degrees of freedom instead of hadronic ones. There is a conventional approach for theoretically calculating b_1 by quark distribution functions convoluted with nucleon momentum distributions in the deuteron including the D-state admixture. According to our experience on the nucleon-spin issue, such a conventional approach for high-energy spin physics would not work. In particular, it is known that b_1 is sensitive to dynamical aspects of constituents with angular momenta. Measurements of b_1 could open a new field of spin physics because this kind of spin physics has not been explored anywhere else. Only experimental information came from the HERMES collaboration; however, their data are not accurate enough to find x dependence of b_1 especially at large x . It is an unique opportunity at JLab to develop this new field of spin physics.”

S. Kumano (KEK and Tsukuba U.)

“I’m glad to hear that b_1 is not forgotten in all the excitement about other spin dependent effects... The hard thing is to distinguish a non-trivial contribution to b_1 (eg. from 6 quark correlations in the deuteron) from the contribution from the deuteron d-wave.”

R. Jaffe (MIT)

“I am particularly interested in signatures of novel QCD effects in the deuteron. The tensor charge could be sensitive to hidden color (non-nucleonic) degrees of freedom at large x . It is also interesting that antishadowing in DIS in nuclei is not universal but depends on the quark flavor and spin. One can use counting rules from PQCD to predict the $x \rightarrow 1$ dependence of the tensor structure function.”

S. Brodsky (SLAC)

“I am certainly interested in the experimental development to find the novel QCD phenomena from the hidden color component of deuteron.”

Chuang-Ryong Ji (SLAC)

2 Existing Data

The HERMES collaboration made the first measurement [5] of the inclusive tensor structure function b_1 in 2005. The experiment explored the kinematic range of $0.001 < x < 0.45$ for $0.5 < Q^2 < 5 \text{ GeV}^2$. An atomic beam source was used to generate a deuterium gas target with high tensor polarization. The HERA storage ring provided 27.6 GeV positrons incident on the internal gas target.

The tensor asymmetry A_{zz} was found to be non-zero by about two sigma for $x < 0.1$, and the tensor structure function b_1 displayed a steep rise as $x \rightarrow 0$. The CK integral was evaluated and found to be

$$\int_{0.0002}^{0.85} b_1(x) dx = 0.0105 \pm 0.0034 \pm 0.0035 \quad (10)$$

which result possibly indicates a breaking of the Close-Kumano sum rule, and consequently a tensor-polarized quark sea.

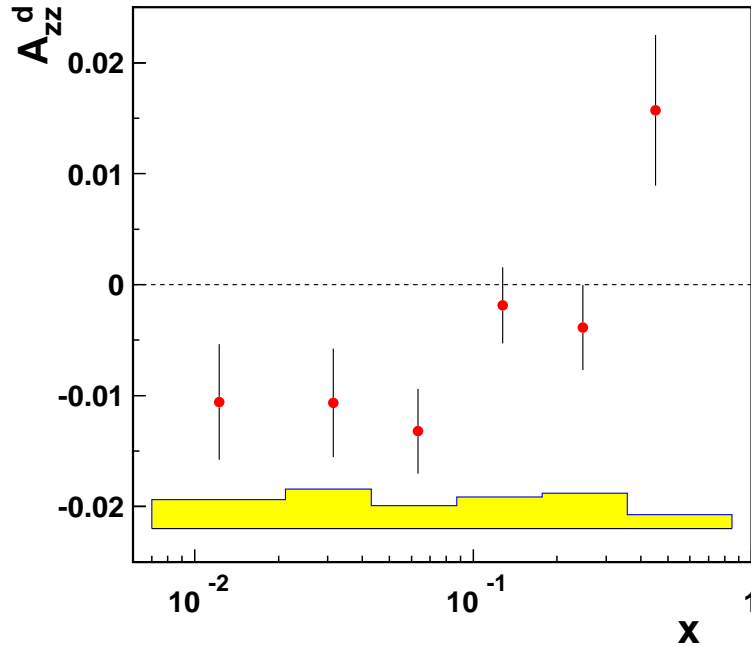


Figure 2: HERMES measurement of the inclusive tensor asymmetry A_{zz} of the deuteron. The error band displays the total systematic uncertainty. *Reproduced from [12].*

As often the case with pioneer measurement, the precision of the results leaves room for ambiguities on the type of phenomena which are responsible for a non-zero value of b_1 . One worry is that HERMES Q^2 values are low at small x (see Fig. 4) where quark structure functions may not be the correct language. In addition the Q^2 coverage in each x -bin is quite wide and could mask any Q^2 -dependence. Indeed, several theoretical models, as for example displayed in Fig. 1, show a significant Q^2 -dependence for $x \leq 0.1$.

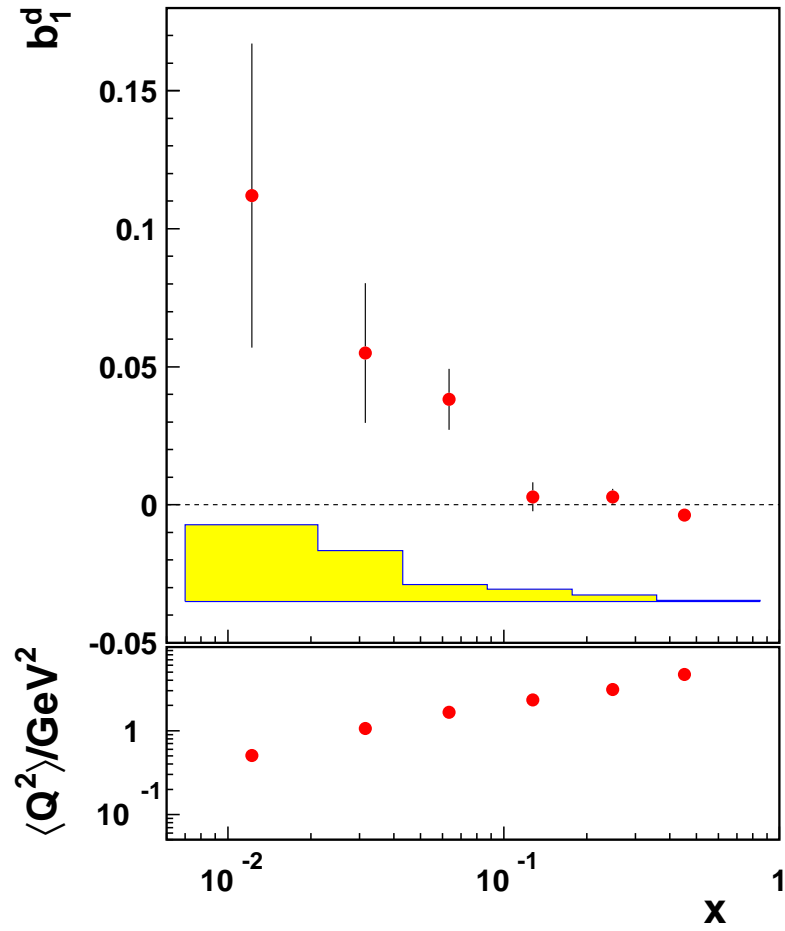


Figure 3: HERMES measurement of the inclusive tensor structure function b_1^d and the average Q^2 for each x -bin. The error band displays the total systematic uncertainty. *Reproduced from [12].*

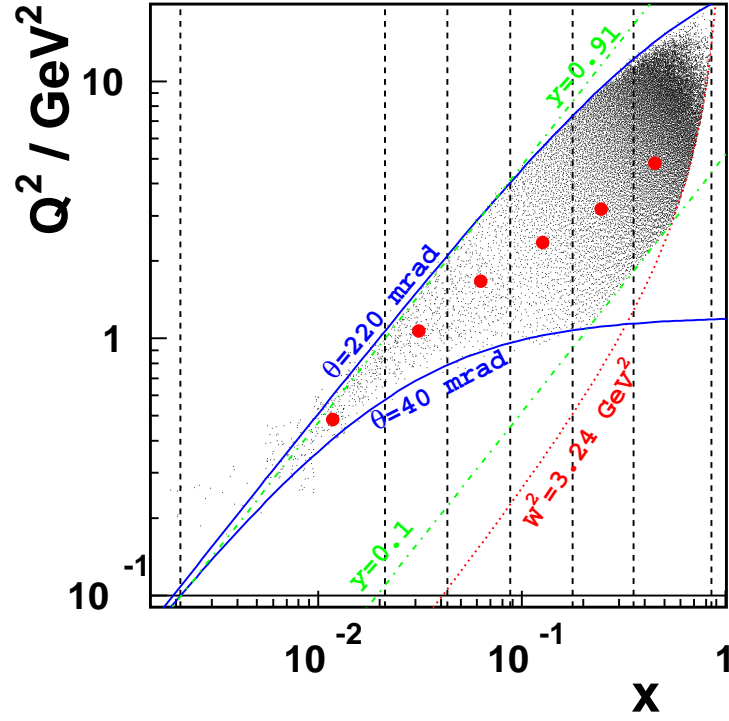


Figure 4: Kinematic coverage of the HERMES measurement. The dashed vertical lines indicate the borders of the bins in x , the big dots their centers of gravity. The solid curves indicate the vertical acceptance of the spectrometer, defined by its aperture. In addition, the kinematic cuts imposed on the variables Q^2 , y and W^2 are shown. The W^2 cut suppresses the nuclear resonance region. *Reproduced from [12].*

3 The Proposed Experiment

We will measure the deuteron tensor asymmetry A_{zz} and extract the leading twist tensor structure function b_1 for $0.05 < x < 0.60$, $1.0 < Q^2 < 5.0 \text{ GeV}^2$ and $W \geq 2.0 \text{ GeV}$. Fig. 8 shows the kinematic coverage available at JLab utilizing an 11 GeV beam, and the Hall A SoLID spectrometer.

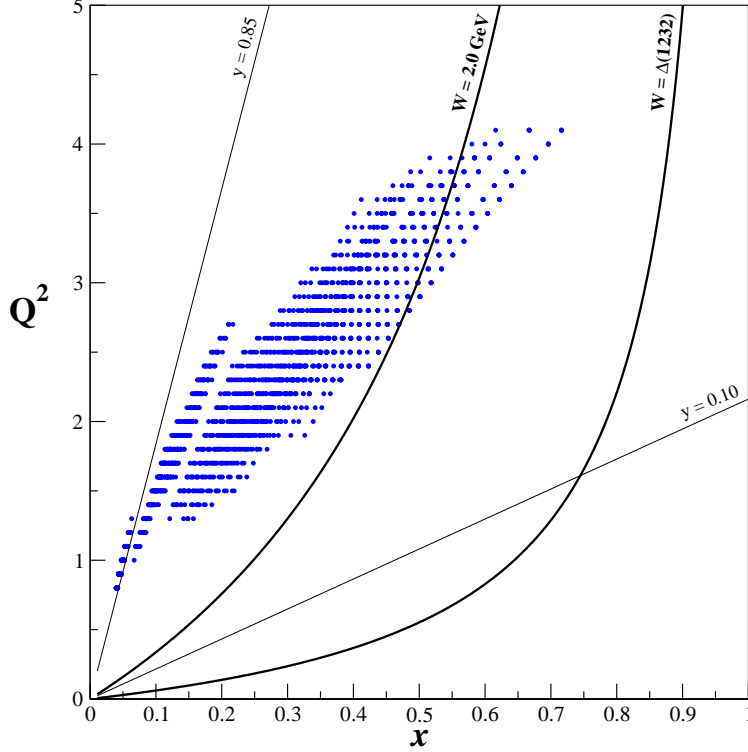


Figure 5: Kinematic coverage for 11 GeV beam in Hall A using the SoLID spectrometer.

The polarized target considered in this letter-of-intent is the solid lithium deuteride (LiD) since it has a better dilution factor than ND_3 . The vector polarization, packing fraction and dilution used in the estimate of the rates are 55%, 0.55 and 0.50 respectively. With an incident electron beam current of 100 nA, the expected deuteron luminosity is $2 \times 10^{35} \text{ cm}^{-2}\text{s}^{-1}$. The acceptance of SoLID was assumed to be $\Delta\Omega = 1.43 \text{ sr}$. The kinematics, physics rates[§], projected statistical uncertainties of A_{zz} and b_1 along with the time necessary to achieve this precision are summarized in Table 2. The projected uncertainties are displayed in Fig. 6. Only rates with kinematics coverage of $W \geq 2.0 \text{ GeV}$ were computed. So 31 days of beam time is needed for production data. This time will be split equally between parallel and perpendicular running. About seven additional days will be needed for calibration, background study and configuration changes.

[§]For this Letter-of-Intent, we took the rates expected from the Hall C HMS and scaled them to the SoLID acceptance $\Delta\Omega = 1.43 \text{ sr}$. A detailed simulation will be performed in a full proposal.

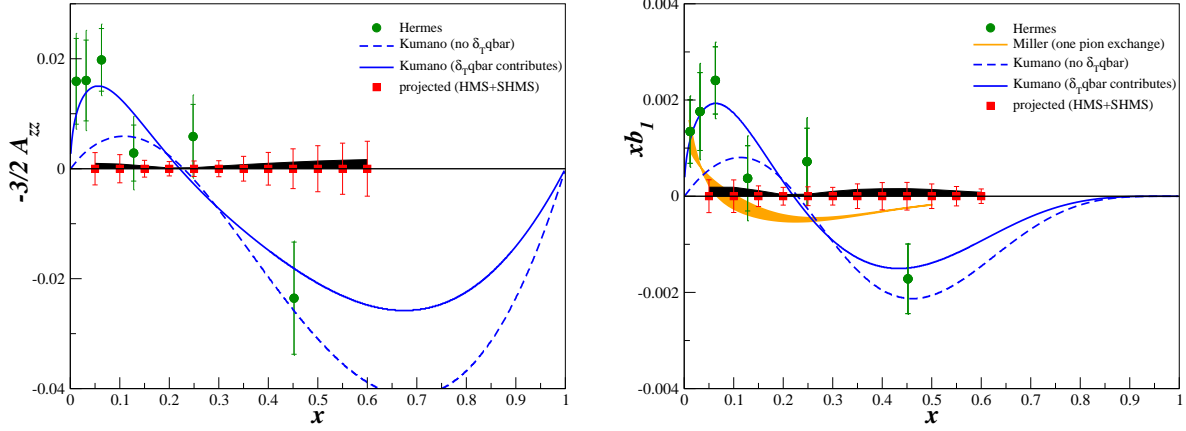


Figure 6: **Left:** Projected precision of the tensor asymmetry A_{zz} with 38 days of beam time. Also shown are the data from Hermes[5] and the calculation from Kumano [6]. **Right:** Corresponding projected precision of the tensor structure function b_1 . In addition, an updated calculation of Ref. [7] from Miller is shown [8]. The black band represents the systematic uncertainty.

3.1 Overhead

In order to calibrate the target NMR system, elastic scattering measurements will be performed at an incident energy of 2.2 GeV. Two days, including the energy pass change, should be sufficient. Measurements of the dilution from the unpolarized materials contained in the target, and of the packing fraction due to the granular composition of the target material will be performed on a ^6Li target and carbon target. A total of 8 hours of data will be needed. Target annealing and target material changes will be performed once a week. Table 1 summarizes the expected overhead. The magnetic field of the target will be rotated from parallel to perpendicular configuration about once a week. Approximately 7 additional days will be needed for calibration, background study and configuration changes.

Table 1: Summary of the overhead

	time (hrs)	number	total time (hrs)
elastic			48.0
dilution			8.0
configuration change	16	4	64.0
beam energy meas.	2.0	2	4.0
BCM calibration	1.0	2	2.0
target annealing	2.5	4	10.0
target material change	4.0	4	16.0

Table 2: Summary of the kinematics and physics rates using Hall A SoLID spectrometer for the measurement.

$\langle x \rangle$	$\langle Q^2 \rangle$ (GeV) ²	$\langle W \rangle$ (GeV)	P_0 (GeV)	θ (deg.)	Rates (kHz)	A_{zz} $\times 10^{-2}$	δA_{zz}^{stat} $\times 10^{-2}$	b_1 $\times 10^{-2}$	δb_1^{stat} $\times 10^{-2}$	time (hours)
0.05	1.0	4.5	0.82	19.1	0.40	-0.98	0.20	3.4	0.68	378
0.10	1.5	3.8	3.37	11.5	4.52	-0.85	0.17	1.7	0.34	44
0.15	2.0	3.5	4.22	11.9	5.58	-0.51	0.10	0.71	0.14	100
0.20	2.0	3.0	5.91	10.1	15.07	-0.14	0.087	0.15	0.092	51
0.25	2.0	2.6	6.93	9.3	31.60	0.19	0.094	-0.16	0.078	21
0.30	2.5	2.6	6.76	10.5	14.69	0.48	0.097	-0.31	0.061	42
0.35	2.5	2.4	7.37	10.1	23.19	0.75	0.15	-0.37	0.073	11
0.40	3.0	2.3	7.18	11.2	10.81	0.99	0.20	-0.35	0.071	14
0.45	3.0	2.2	7.61	10.9	14.79	1.2	0.24	-0.32	0.064	7
0.50	3.5	2.1	7.44	11.9	8.19	1.4	0.28	-0.26	0.051	9
0.55	4.5	2.2	6.84	14.1	2.62	1.6	0.31	-0.18	0.037	23
0.60	5.0	2.1	6.76	14.9	1.46	1.7	0.33	-0.13	0.025	36

3.2 Background

The pion background has not been estimated yet for this measurement, but should be comparable to other proposed DIS measurements with SoLID. A careful study of the background will be performed in a full proposal.

3.3 Experimental Method

Following Ref. [3] it is possible to measure the asymmetry A_{zz} by taking the difference of parallel and perpendicular cross sections with unpolarized beam:

$$\frac{\frac{d^2\sigma_{\parallel}}{d\Omega dE'} - \frac{d^2\sigma_{\perp}}{d\Omega dE'}}{\frac{d^2\sigma_{\parallel}}{d\Omega dE'} + 2\frac{d^2\sigma_{\perp}}{d\Omega dE'}} = -\frac{1}{2}\left(1 - \frac{3}{2}H^2\right)A_{zz}, \quad (11)$$

where $H^2 = (P + 2)/3$ is the target spin projection along the beam and P is the target polarization. The polarized cross sections $d^2\sigma_{\parallel}/d\Omega dE'$ and $d^2\sigma_{\perp}/d\Omega dE'$ can be extracted from data collected by scattering an unpolarized electron beam off a spin-1 target polarized longitudinally and perpendicularly to the electron beam direction. The tensor structure function b_1 can then be extracted as follows:

$$\frac{b_1}{F_1} = -\frac{3}{2}A_{zz} \quad (12)$$

From Eq. 11, the beam time needed to achieve an absolute uncertainty of δA_{zz} can be deduced and is expressed as follows:

$$T = \frac{32}{9P_{zz}^2 R_D f (P_{zz} \delta A_{zz})^2} \quad (13)$$

with R_D is the deuteron rate, f the dilution factor and P_{zz} the tensor polarization.

Polarimetry	8%
Dilution/packing fraction	5%
Computer deadtime	0.5%
Charge measurement	0.5%
Energy measurement	0.05%
Radiative corrections	5%
Total Systematic Uncertainty	11%

Table 3: Relative systematic uncertainties.

3.4 Systematic Uncertainties

In this Letter-of-Intent, we consider using a model for the unpolarized structure function F_1 needed to extract b_1 from Eq. 17. So an additional systematic uncertainty will have to be taken into account in the extraction of b_1 from the A_{zz} measurement.

3.5 Alternate Methodology

In addition to the experimental approach considered in this Letter-of-Intent, we have two other options which we will explore further in preparation for a full proposal:

1. measuring the tensor structure function b_1 with a longitudinally polarized target using the cross section method suggested in Ref. [3];
2. measuring the tensor asymmetry A_{zz} using the HERMES method [12], with only a longitudinally polarized target.

We are also exploring other forms of accessing A_{zz} that don't rely on A_2^d being negligible, like HERMES assumed.

3.6 Polarized Target

This experiment will require the installation of the UVa polarized target operated in longitudinal and also transverse mode. Transverse polarization requires operation of an upstream chicane to ensure proper transport through the target magnetic field. The target is typically operated with a specialized slow raster, and beamline instrumentation capable of characterizing the low current 50-100 nA beam. All of these requirements have been met previously in Hall C, and will be soon implemented also in Hall A for the E08-027/E08-007 run in 2011. The UVa polarized target (see Fig. 7), has been successfully used in experiments E143, E155, and E155x at SLAC, and E93-026, E01-006 and E07-003 at JLab. In 2011, the same target will be utilized in experiments E08-027 and E08-007. A similar target was used in Hall B for the EG1, EG4 and DVCS experiments, although Hall B does not at present have the facilities necessary for transverse polarization.

The UVa target operates on the principle of Dynamic Nuclear Polarization, to enhance the low temperature (1 K), high magnetic field (5 T) polarization of solid materials by microwave pumping. The polarized target assembly contains several target cells of 3.0 cm length that can be selected individually by remote control to be located in the uniform field region of a superconducting Helmholtz pair. The permeable target cells are immersed in a vessel filled with liquid Helium and maintained at 1 K by use of a high power

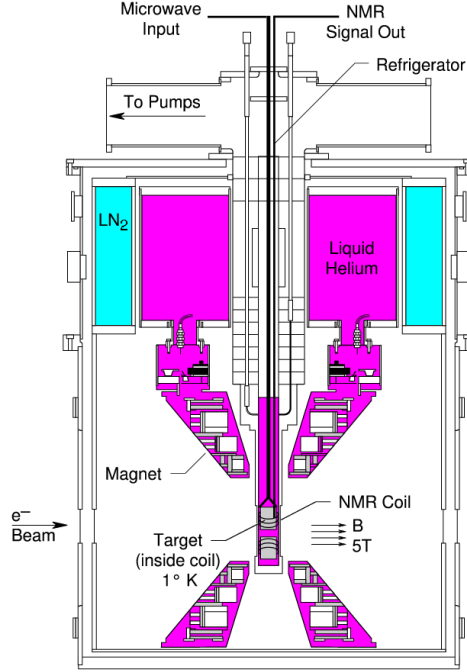


Figure 7: Cross section view of the polarized target

evaporation refrigerator. The coils have a 50° conical shaped aperture along the beam axis which allow for unobstructed forward scattering.

The target material is exposed to 140 GHz microwaves to drive the hyperfine transition which aligns the nucleon spins. The heating of the target by the beam causes a drop of a few percent in the polarization, and the polarization slowly decreases with time due to radiation damage. Most of the radiation damage can be repaired by annealing the target at about 80 K, until the accumulated dose reached is greater than about $17 \times 10^{15} \text{ e}^-/\text{cm}^2$, at which time the target material needs to be replaced. The luminosity of the polarized material in the uniform field region is approximately $85 \times 10^{33} \text{ cm}^{-2} \text{ Hz}$.

Tensor Polarization

When a spin 1 system such as the deuteron is subjected to a magnetic field along the z-axis, the Zeeman interaction gives rise to three magnetic sublevels $I_z = +1, 0, -1$ with population fractions p_+, p_-, p_0 , respectively. These populations are described by both a vector polarization,

$$\begin{aligned} P_z &= \langle I_z / I \rangle \\ &= (p_+ - p_-) + (p_0 - p_+) = p_+ - p_- \end{aligned} \quad (14)$$

and a tensor polarization [13]:

$$\begin{aligned} P_{zz} &= \langle 3I_z^2 - I(I+1) \rangle / I^2 \\ &= (p_+ - p_-) - (p_0 - p_-) = 1 - 3p_0 \end{aligned} \quad (15)$$

which are subject to the overall normalization $p_+ + p_- + p_0 = 1$. In the case of deuteron spins in thermal equilibrium with the solid lattice, and neglecting the small quadrupole interaction [13], the tensor polariza-

tion is related to the vector polarization via:

$$P_{zz} = 2 - \sqrt{4 - 3P_z^2} \quad (16)$$

This relation allows calculation of a target's tensor polarization once the vector polarization has been determined from standard NMR techniques. Vector polarizations can be determined by analyzing NMR line-shapes as described in [14] with a typical 7% relative uncertainty, or by comparison of the NMR response to the known thermal equilibrium (TE) polarization.

The DNP technique produces deuteron vector polarizations of up to 60% in ND₃ and 64% in LiD [15], which corresponds to tensor polarizations of approximately 30%. Tensor polarizations of 22% have been achieved in previous experiments [13] using standard solid polarized ammonia targets. At the University of Virginia and the University of New Hampshire, we are pursuing techniques to enhance the tensor polarization by directly stimulating transitions to/from the $M_s = 0$ state. The UVa group had some initial success in obtaining enhanced tensor polarizations via RF pumping, although the method was not pursued due to lack of need for tensor polarized targets at the time of the study. Another method entails simultaneously pumping the paramagnetic centers with two independent microwave frequencies, which requires careful isolation of the respective microwave cavities. As this work is on-going, the rates in this proposal assume only tensor polarizations that have been demonstrated previously.

4 Summary

This experiment will require 38 days of beam time in order to perform a precision measurement of b_1^d using a longitudinally polarized deuteron (LiD) target, together with the Hall A SoLID spectrometer.

A Feasibility Study in Hall C with the HMS and SHMS Spectrometers

We studied the feasibility of a measurement on the leading twist tensor structure function b_1 for $0.15 < x < 0.55$, $1.5 < Q^2 < 4.2 \text{ GeV}^2$ and $W \geq 2.0 \text{ GeV}$. Fig. 8 shows the kinematic coverage available at JLab utilizing an 11 GeV beam, and the Hall C HMS and SHMS spectrometers at forward angle.

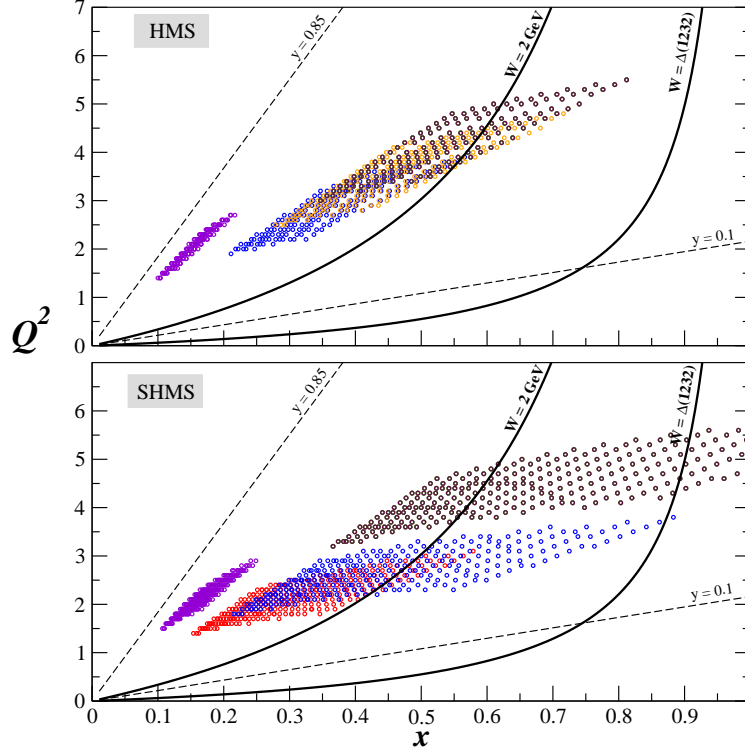


Figure 8: Kinematic coverage for 11 GeV beam in Hall C using the HMS and SHMS.

The polarized target considered in this letter-of-intent is the solid lithium deuteride (LiD) since it has a better dilution factor than ND_3 . The vector polarization, packing fraction and dilution used in the estimate of the rates are 55%, 0.55 and 0.50 respectively. With an incident electron beam current of 100 nA, the expected deuteron luminosity is $2 \times 10^{35} \text{ cm}^{-2} \text{ s}^{-1}$. The momentum bite and the acceptance were assumed to be $\Delta P = \pm 8\%$ and $\Delta \Omega = 6.5 \text{ msr}$ for the HMS, and $\Delta P = {}^{+20\%}_{-8\%}$ and $\Delta \Omega = 4.4 \text{ msr}$ for the SHMS. For the choice of the kinematics, special attention was taken onto the angular and momentum limits of the spectrometers: for the HMS, $10.5^\circ \leq \theta \leq 85^\circ$ and $1 \leq P_0 \leq 7.3 \text{ GeV}/c$, and for the SHMS, $5.5^\circ \leq \theta \leq 40^\circ$ and $2 \leq P_0 \leq 11 \text{ GeV}/c$. In addition, the opening angle between the spectrometers is physically constrained to be larger than 17.5° . The kinematics, rates, projected statistical uncertainties of A_{zz} and b_1 along with the time necessary to achieve this precision are summarized in Table 5. The projected uncertainties are displayed in Fig. 9. Only rates with kinematics coverage of $W \geq 2.0 \text{ GeV}$ were computed. A total of 24 days of beam time is needed for production data.

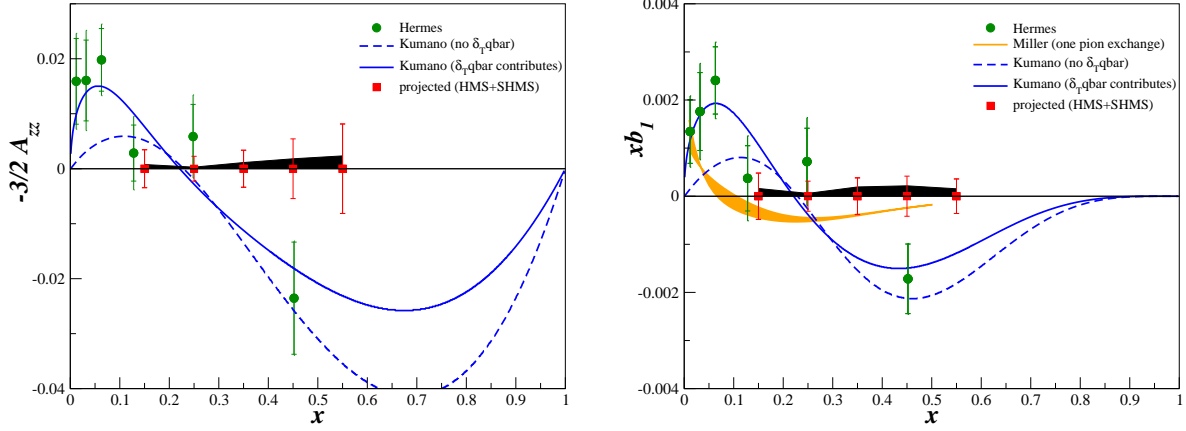


Figure 9: **Left:** Projected precision of the tensor asymmetry A_{zz} with 30 days of beam time. Also shown are the data from Hermes[5] and the calculation from Kumano [6]. **Right:** Corresponding projected precision of the tensor structure function b_1 . In addition, an updated calculation of Ref. [7] from Miller is shown [8]. The black band represents the systematic uncertainties but a 60% uncertainty should be added from the contribution of F_1 in the measured cross sections.

A.1 Overhead

In order to calibrate the target NMR system, elastic scattering measurement will be performed at an incident energy of 2.2 GeV. Two days, including the energy pass change, should be sufficient. The measured cross sections will need to be corrected by the dilution from the unpolarized materials contained in the target and by the packing fraction due to the granular composition of the target material. In order to evaluate these two factors, a total of 8 hours of data will be taken on a lithium target and on a carbon target. Target annealing and target material change will be done once a week. Table 4 summarizes the expected overhead. About 4 additional days will be needed for calibration, background study and configuration changes.

Table 4: Summary of the overhead

	time (hrs)	number	total time (hrs)
elastic			48.0
dilution			8.0
configuration change	0.5	4	2.0
beam energy meas.	2.0	2	4.0
BCM calibration	1.0	2	2.0
target annealing	2.5	4	10.0
target material change	4.0	4	16.0

Table 5: Summary of the kinematics and rates using Hall C HMS (top part of the table) and SHMS (bottom part of the table) spectrometers for the measurement.

$\langle x \rangle$	$\langle Q^2 \rangle$ (GeV) ²	$\langle W \rangle$ (GeV)	P_0 (GeV)	θ (deg.)	Rates (Hz)	A_{zz} $\times 10^{-2}$	δA_{zz}^{stat} $\times 10^{-2}$	b_1 $\times 10^{-2}$	δb_1^{stat} $\times 10^{-2}$	time (hours)
0.15	2.0	3.5	4.22	11.9	6.34	-0.51	0.23	0.71	0.32	285
0.35	2.8	2.5	6.93	11.0	14.77	0.75	0.22	-0.36	0.11	128
0.45	3.5	2.3	7.04	12.2	8.02	1.2	0.36	-0.31	0.93	91
0.55	4.2	2.1	7.11	13.3	4.03	1.6	0.54	-0.19	0.065	80
0.15	2.0	3.5	4.22	11.9	7.03	-0.51	0.23	0.71	0.32	257
0.25	2.0	2.6	6.93	9.3	41.77	0.19	0.15	-0.16	0.13	101
0.35	2.5	2.4	7.37	10.1	21.87	0.75	0.22	-0.37	0.11	86
0.55	4.2	2.1	7.11	13.3	2.43	1.6	0.54	-0.19	0.065	133

A.2 Background

The pion background has not been estimate yet for this measurement, but the detector package of the HMS and SHMS should provide a sufficient particle identification efficacy.

A.3 Experimental Method

Following Ref. [3] it is possible to isolate the tensor structure function b_1 from the parallel cross section expressed as follows:

$$\frac{d^2\sigma_{\parallel}}{dx dy} = \frac{e^4 ME}{2\pi Q^4} [1 + (1 - y)^2] [xF_1(x) + (\frac{2}{3} - H^2)xb_1(x)] \quad (17)$$

where $H^2 = (P + 2)/3$ is the target spin projection along the beam and P is the target polarization. The polarized cross sections $d^2\sigma_{\parallel}/d\Omega dE'$ are measured by scattering an unpolarized electron beam off a spin-1 target polarized longitudinally to the electron beam direction.

From Eq. 17, the beam time needed to achieve an absolute uncertainty of δA_{zz} can be deduced and is expressed as follows:

$$T = \frac{1}{R_D f (P_{zz} \delta A_{zz})^2} \quad (18)$$

where R_D is the deuteron rate, f the dilution factor and P_{zz} the tensor polarization. The expression of the tensor asymmetry A_{zz} can be found in Eq. 12.

A.4 Conclusion

The main concern of this method is the systematic uncertainty from F_1 . Since F_1 is about 30 times larger than b_1 (at $x = 0.45$), a 2% uncertainty in F_1 will translate into 60% systematic uncertainty in b_1 which is larger than HERMES uncertainty. We believe any precision measurement will have to come from the asymmetry or ratio method.

References

- [1] A. Pais, Phys. Rev. Lett. **19**, 544 (1967).
- [2] L. L. Frankfurt and M. I. Strikman, Nucl. Phys. **A405**, 557 (1983).
- [3] P. Hoodbhoy, R. L. Jaffe, and A. Manohar, Nucl. Phys. **B312**, 571 (1989).
- [4] K. Bora and R. L. Jaffe, Phys. Rev. **D57**, 6906 (1998).
- [5] A. Airapetian *et al.*, Phys. Rev. Lett. **95**, 242001 (2005).
- [6] S. Kumano, Phys. Rev. **D82**, 017501 (2010).
- [7] G. A. Miller, In *Stanford 1989, Proceedings, Electronuclear physics with internal targets* 30-33. .
- [8] G. A. Miller, private communication, to be published.
- [9] P. J. Sutton, A. D. Martin, R. G. Roberts, and W. J. Stirling, Phys. Rev. **D45**, 2349 (1992).
- [10] H. Khan and P. Hoodbhoy, Phys. Rev. **C44**, 1219 (1991).
- [11] F. E. Close and S. Kumano, Phys. Rev. **D42**, 2377 (1990).
- [12] C. Riedl, Ph. D thesis, DESY-THESIS-2005-027 (2005).
- [13] W. Meyer *et al.*, Nucl. Instrum. Meth. **A244**, 574 (1986).
- [14] C. Dulya *et al.*, Nucl. Instrum. Meth. **A398**, 109 (1997).
- [15] S. L. Bueltmann *et al.*, Nucl. Instrum. Meth. **A425**, 23 (1999).